8. Finite Element Method (FEM) in Mechanics

8.1. Introduction

The focus of the previous presentation of FEM theory was mainly on its application to electromagnetic field analysis. As we will see, to qualitatively describe the functioning of micro-electro-mechanical systems (MEMS) we have to perform a mechanical analysis as well. Therefore, we will now give a short review of FEM application to mechanics with the focus on subjects related to MEMS. Since we have already learned the fundamental theory of FEM, we will skip this part here and present only the topics that are specific to mechanics.

8.2. Equations for 2D Solids

For simplicity reasons we will only present the details of 2D mechanics of materials in this section. The scope of mechanics of materials is the development of methods for computation and analysis of stresses (the intensity of forces) and strains (the severity of deformations) as well as the load-carrying capabilities of components and structures [1, 2].
Solid bodies exhibit two types of deformations: *elastic* and *plastic*. Elastic deformations disappear when the load that is causing the deformation is removed, i.e. the body resumes its initial shape. Plastic deformations on the other hand are permanent and remain even when the load that caused them is removed, i.e. the body does not resume its initial shape. All solid bodies exhibit both types of deformations under loading, often beginning with purely elastic deformations, ending with largely plastic deformations, and experiencing a combination of the two in between. An elastic solid is a theoretical solid that only exhibits elastic deformations and is a good approximation of many materials under relatively small loads.
We will focus our analysis on elastic solids and structures. Moreover, our analysis will only consider problems with very small deformations that show a linear relationship between the deformation and corresponding load.

8.2.1 Stress and Strain

Let us consider a continuous 2D solid (infinite length in z-direction) with a surface S and a boundary Γ as depicted in Figure 8.1a. As one can see the boundary of our solid body can be divided into two types: boundaries along which the external forces are predefined (Γ_{f1} and Γ_{f2}) and boundaries with prescribed displacements (Γ_{d1} and Γ_{d2}).

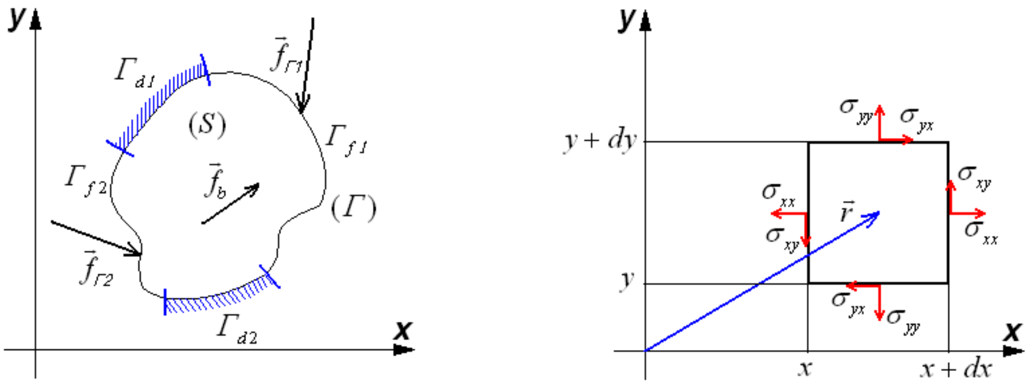

(8.a) (8.b)

Figure 8.1. 2D solid body is depicted; The load of the body is shown as the body force ($\vec{f}_b$) and the boundary force ($\vec{f}_{\Gamma 1}$ and $\vec{f}_{\Gamma 2}$).

The body is loaded with a body force ($\vec{f}_b$) and boundary force ($\vec{f}_{\Gamma 1}$ and $\vec{f}_{\Gamma 2}$) [2]. The intensity of force in mechanics is called stress and its definition is always related to the corresponding surface on which the force acts. Therefore it is possible to distinguish a normal stress and a shear stress [2].
A normal stress σ is defined as an elemental normal force dF acting on an elemental area dA [2]:

$$\sigma = \lim_{\Delta A \to 0} \frac{\Delta F}{\Delta A} = \frac{dF}{dA} \tag{8.1}$$

The SI unit for normal stress is Newton over square meter, i.e. Pascal[1] [$N/m^2=Pa$].
A tangential or shear stress τ is defined as an elemental tangential or shear force dV acting on an elemental area dA [2]:

$$\tau = \lim_{\Delta A \to 0} \frac{\Delta V}{\Delta A} = \frac{dV}{dA} \tag{8.2}$$

The SI unit for shear stress is also Newton over square meter, i.e. Pascal[1] [$N/m^2=Pa$].
At any point in the solid body one can define an “infinitely” small rectangular surface (2D) as illustrated in Figure 8.1b. On each boundary of the surface we have a normal and shear stress component. Therefore the stress itself is a tensor and in the 2D case has 4 components [2]:

$$\ddot{\sigma} = \begin{bmatrix} \sigma_{xx} & \sigma_{xy} \\ \sigma_{yx} & \sigma_{yy} \end{bmatrix} \tag{8.3}$$

where the first letter of the subscript represents the boundary on which the stress is acting and the second letter represents the direction of the stress. Consequently, if both letters are the same (either *xx* or *yy*) we have a normal stress. Otherwise, we speak about shear stress. This convention is helpful to have a clear and unambiguous notation, although it is in disagreement with equation (8.2) where (for traditional reasons) we have denoted the shear stress as τ.
If we define the axis in the middle of the surface element shown in Figure 8.1b perpendicular to the surface plane and if we take moments of forces about the axis at equilibrium (sum of moments equals to zero), it is very simple to show the following:

$$\sigma_{xy} = \sigma_{yx} \tag{8.4}$$

i.e. the stress tensor (8.3) is symmetric. Hence, the stress tensor is usually written in the following vector form [1, 2]:

$$\{\sigma\} = \{\sigma_{xx} \quad \sigma_{yy} \quad \sigma_{xy}\}^T \tag{8.5}$$

When forces act on a solid material they deform it; the severity of the deformation depends on the intensity of the force as well as on the material properties. The severity of a deformation is called *strain,* having separate definitions for volumetric change and angular distortion of a solid body.

---

[1] Blaise Pascal (1623–1662), French mathematician and philosopher.

A *normal strain* is defined as the elemental elongation of a line segment under an axial force over the elemental original or gage length [2]:

$$\varepsilon = \lim_{\Delta L \to 0} \frac{\Delta e}{\Delta L} = \frac{de}{dL} \approx \frac{e}{L_0} \tag{8.6}$$

where L_0 is the initial length of a given line segment and *e* is the change in length of the line segment, i.e. the deformation. As one can see in (8.6), the ratio of elemental deformation to elemental length can be approximated for small deformations with the ratio between the deformation and the initial length.

Shear strain is defined in a similar way as for normal strain. This is again the ratio of deformation to original dimension but the deformation and force is now perpendicular to the axis of the given line segment [2]:

$$\gamma = \lim_{\Delta L \to 0} \frac{\Delta \delta}{\Delta L} = \frac{d\delta}{dL} \approx \frac{\delta}{L_0} = \tan \alpha \tag{8.7}$$

Definitions (8.6) and (8.7) are considering the deformation of the line segment along and perpendicular to its axis. In the 2D case it is clear that the vector representation of the stress corresponds to a similar representation of the strain [2]:

$$\{\varepsilon\} = \{\varepsilon_{xx} \quad \varepsilon_{yy} \quad \varepsilon_{xy}\}^T \tag{8.8}$$

where the subscript notation has the same meaning as for stress. In order to represent the deformation of the body it is useful to define the displacement functions $u = u(x, y)$ and $v = v(x, y)$ in the *x* and *y* directions respectively. Having definitions (8.6) and (8.7) we can write equations for the strain components with respect to the displacements in the following way [2]:

$$\varepsilon_{xx} = \frac{\partial u}{\partial x},\ \varepsilon_{yy} = \frac{\partial v}{\partial y},\ \varepsilon_{xy} = \frac{\partial v}{\partial x} + \frac{\partial u}{\partial y} \tag{8.9}$$

or in a matrix form:

$$\{\varepsilon\} = [L] \cdot \{U\} \tag{8.9'}$$

where:

$$\{\varepsilon\} = \{\varepsilon_{xx} \quad \varepsilon_{yy} \quad \varepsilon_{xy}\}^T,\ \{U\} = \{u \quad v\}^T,\ [L] = \begin{bmatrix} \frac{\partial}{\partial x} & 0 \\ 0 & \frac{\partial}{\partial y} \\ \frac{\partial}{\partial y} & \frac{\partial}{\partial x} \end{bmatrix} \tag{8.9''}$$

8.2.2. Generalized stress-strain expression – Hooke's law

To make a relation between stress and strain in the case of a 2D solid body it is necessary to distinguish two different situations that both can be described with the same equations (8.9', 8.5, 8.8) in the x0y plane. In the first case, our 2D solid body is very thin in the *z* direction compared to its dimensions in the *x* and *y* direction. In this case the external forces are applied only in the *x-y* plane and stresses are equal to zero in the *z* direction. Therefore such a solid is called a *plain stress* solid [1]. It is important to notice that the strain ε_{zz} in this case is not equal to zero in general, while ε_{xz} and ε_{yz} are zero. It is worth mentioning that the strain ε_{zz} does not appear in the equation of 2D solid body (8.9') and it can be extracted using the equation (8.12') after the in-plane stress (in the form (8.5)) has been obtained.
An alternative to the previous case is a solid with the length in the *z* direction much larger than its size in the *x-y* plane. This solid is called a *plain strain* solid [1]. The external forces are applied evenly along the z axis in this case and the displacement in the z direction is equal to zero (constrained). Hence the strain components in the *z* direction are zero. The stress component σ_{zz} is not necessarily equal to zero here, while σ_{xz} and σ_{yz} are zero. Similar to the previous case the stress σ_{zz} does not appear in the equation of 2D solid body (8.9') and it can be extracted using the equation (8.12') after the in-plane stress (in the form (8.5)) has been obtained.
The relation between stress and strain was experimentally discovered in the 17th century by Robert Hooke[2] and is therefore called Hooke's law. It can be written in the following matrix form:

$$\{\sigma\} = [C] \cdot \{\varepsilon\} \tag{8.10}$$

where $[C]$ is a matrix of material constants having the following forms [2]:

$$[C] = \frac{E}{1-\nu^2} \begin{bmatrix} 1 & \nu & 0 \\ \nu & 1 & 0 \\ 0 & 0 & (1-\nu)/2 \end{bmatrix} \text{(Plane stress)} \tag{8.11}$$

$$[C] = \frac{E(1-\nu)}{(1+\nu)(1-2\nu)} \begin{bmatrix} 1 & \nu/(1-\nu) & 0 \\ \nu/(1-\nu) & 1 & 0 \\ 0 & 0 & (1-2\nu)/[2(1-\nu)] \end{bmatrix} \text{(Plane strain)} \tag{8.12}$$

in which *E* is Young's modulus[3] and ν is Poisson's ratio[4].
Hooke's law written in 3D general case for fully anisotropic material has the following form [1]:

[2] Robert Hooke (8.1635-1703), English mathematician.
[3] Young's modulus is also known as the modulus of elasticity; it is a measure of the stiffness of a given material and it is defined as the ratio of stress with strain (the SI unit is $N/m^2=Pa$)
[4] Poisson's ration is defined as a measure of the tendency of material stretched in one direction to shrink in the remaining two directions.

$$\begin{Bmatrix} \sigma_{xx} \\ \sigma_{yy} \\ \sigma_{zz} \\ \sigma_{yz} \\ \sigma_{xz} \\ \sigma_{xy} \end{Bmatrix} = \begin{bmatrix} c_{11} & c_{12} & c_{13} & c_{14} & c_{15} & c_{16} \\ & c_{22} & c_{23} & c_{24} & c_{25} & c_{26} \\ & & c_{33} & c_{34} & c_{35} & c_{36} \\ & & & c_{44} & c_{45} & c_{46} \\ & Symm. & & & c_{55} & c_{56} \\ & & & & & c_{66} \end{bmatrix} \begin{Bmatrix} \varepsilon_{xx} \\ \varepsilon_{yy} \\ \varepsilon_{zz} \\ \varepsilon_{yz} \\ \varepsilon_{xz} \\ \varepsilon_{xy} \end{Bmatrix} \tag{8.12'}$$

where $c_{ij} = c_{ji}$ are altogether 21 independent material constants [1].

8.2.3. Dynamic Equilibrium Equations

To formulate the dynamic equilibrium equations let us go back to an infinitely small rectangular block of the 2D solid body presented in Figure 8.1b. An equilibrium of forces acting on this small block is required in all directions. Since we are considering dynamics, the inertial forces have to be taken into account. Thus the equilibrium of forces in the x direction reads:

$$\left(\sigma_{xx} + d\sigma_{xx}\right) \cdot dy - \sigma_{xx} \cdot dy + \left(\sigma_{yx} + d\sigma_{yx}\right) \cdot dx - \sigma_{yx} \cdot dx + f_x' \cdot dx \cdot dy = \rho' \cdot \ddot{u} \cdot dx \cdot dy \tag{8.13}$$

where dz is omitted ($dz = 1$ in 2D) and the other parameters are as follows:

$\rho'(kg/m^2)$	- body mass density of the 2D solid body
$f_x'\left(N/m^2\right)$	- external body force density (x-component)
$\ddot{u}$	- second time derivative of the displacement in the x direction
$\rho' \cdot \ddot{u} \cdot dx \cdot dy$	- inertial force

It is important to notice:

$$d\sigma_{xx} = \frac{\partial \sigma_{xx}}{\partial x} \cdot dx\,,\; d\sigma_{yx} = \frac{\partial \sigma_{yx}}{\partial y} \cdot dy \tag{8.14}$$

By using (8.14), equation (8.13) can be written in a more compact form:

$$\frac{\partial \sigma_{xx}}{\partial x} + \frac{\partial \sigma_{yx}}{\partial y} + f_x' = \rho' \cdot \ddot{u} \tag{8.15}$$

Apparently, similar to (8.15) the equilibrium of forces in the y direction can be written as:

$$\frac{\partial \sigma_{yy}}{\partial y} + \frac{\partial \sigma_{xy}}{\partial x} + f_y' = \rho' \cdot \ddot{v} \tag{8.16}$$

Equations (8.15) and (8.16) written in matrix form become:

$$\begin{bmatrix} \frac{\partial}{\partial x} & 0 & \frac{\partial}{\partial y} \\ 0 & \frac{\partial}{\partial y} & \frac{\partial}{\partial x} \end{bmatrix} \cdot \begin{Bmatrix} \sigma_{xx} \\ \sigma_{yy} \\ \sigma_{xy} \end{Bmatrix} + \begin{Bmatrix} f_x' \\ f_y' \end{Bmatrix} = \rho' \cdot \begin{Bmatrix} \ddot{u} \\ \ddot{v} \end{Bmatrix} \tag{8.17}$$

By using the notation given by equations (8.5) and (8.9''), it is possible to write (8.17) in a more compact matrix form:

$$[L]^T \cdot \{\sigma\} + \{f_b\} = \rho' \cdot \{\ddot{U}\} \tag{8.18}$$

By introducing Hooke's law (8.10) and equation (8.9') into (8.18), the dynamic equilibrium equation in an appropriate form is obtained:

$$[L]^T \cdot [C] \cdot [L] \cdot \{U\} + \{f_b\} = \rho' \cdot \{\ddot{U}\} \tag{8.19}$$

Equation (8.19) is the general form of the dynamic equilibrium equation written in matrix form. If the loads acting on a solid body are static then the static analysis of the solid is needed. The static equilibrium equation can easily be obtained from (8.19) by dropping the dynamic term (the second time derivative):

$$[L]^T \cdot [C] \cdot [L] \cdot \{U\} + \{f_b\} = 0 \tag{8.20}$$

8.2.4. Boundary Conditions

As we have already mentioned while describing the distinction of the 2D solid body's boundaries in Figure 8.1a, it is possible to distinguish two main types of boundary conditions (BCs):

1. Displacement boundary conditions (essential or Dirichlet's),
2. Force boundary conditions (natural or Neumann's).

The displacement BC is used to describe a support or constraint on the solid body. Thus, the prescribed displacement values are almost always equal to zero (homogenous BCs). This BC can be written in the following form [1]:

$$u(x,y) = \bar{u}(x,y)\,,\; v(x,y) = \bar{v}(x,y)\,,\; (x,y) \in \Gamma_d \tag{8.21}$$

where $\bar{u}$ and $\bar{v}$ are known functions.
The force BC is used to describe a force or load acting on the body's boundary. In stress vector notation this BC can be written as follows [1]:

$$[n] \cdot \{\sigma\} = \{\bar{t}\} \tag{8.22}$$

where the matrix $[n]$ has the form:

$$[n]=\begin{bmatrix} n_x & 0 & n_y \\ 0 & n_y & n_x \end{bmatrix} \tag{8.23}$$

where n_i ($i = x, y$) are components of the outward normal on the boundary and the vector $\{\bar{t}\}$ is known.

8.3. FEM Discretization

The system of partial differential equations in (8.20) are the so-called *strong forms* of the governing system of equations for solid bodies [2]. The name strong form comes from the strong requirements on the field continuity. In addition, our auxiliary interpolation functions that represent the unknown field have to be differentiable up to the order of the PDEs. The task to obtain the solution of such a strong form appears to be very difficult for practical engineering problems. As we have already shown with the FEM application to the computation of electromagnetic fields, it is much more convenient to use a so called *equivalent integral form* or a *weak form*. The weighted residual method for obtaining an equivalent integral form has previously been described in detail. The minimum energy principle, as an alternative, was also mentioned. A similar approach to construct a weak from is used in mechanics as well. Namely, Hamilton's principle is widely accepted [2]:

"Of all the admissible time histories of displacement the most accurate solution makes the Lagrangian functional a minimum."

An admissible displacement must satisfy the following conditions:

1. the compatibility equations,
2. the essential or the kinematic boundary conditions,
3. the conditions at initial (t_1) and final time (t_2).

In mathematical form Hamilton's principle can be written as follows [1]:

$$\delta\int_{t_1}^{t_2}\Im\cdot dt=0 \tag{8.24}$$

where:

δ	- variation operator,
$\Im = T - \Pi + W_f$	- Lagrangian functional,
$T=\frac{1}{2}\int\limits_{(S)}\rho\{\dot{U}\}^T\{\dot{U}\}dS$	- kinetic energy,
$\Pi=\frac{1}{2}\int\limits_{(S)}\{\varepsilon\}^T\{\sigma\}dS=\frac{1}{2}\int\limits_{(S)}\{\varepsilon\}^T[C]\{\varepsilon\}dS$	- strain energy (potential energy),
$W_f=\int\limits_{(S)}\{U\}^T\{f_b\}dS+\int\limits_{(\Gamma)}\{U\}^T\{f_\Gamma\}dS_\Gamma$	- work of external forces.

Since we have already seen the details of the FEM algorithm we will now only briefly describe a few specific points of FEM application to 2D mechanics.

According to equations (8.19) and (8.20), the unknown function in our mechanical analysis is the displacement. By following the integral contributions approach presented before, the interpolation of the displacement function will be defined on the elemental level, i.e. in the local coordinate system of an element [2]:

$$\left\{U^e\right\}(x,y) = \sum_{i=1}^{n_d} \left[N_i\right](x,y) \cdot \left\{d_i\right\} = \left[N\right](x,y) \cdot \left\{d_e\right\} \tag{8.25}$$

where the superscript *e* represents the function valid on the *e*th element, n_d is the number of nodes of the element (3 for triangles and 4 for quadrilaterals), $\left\{d_i\right\} = \left\{u_i \quad v_i\right\}^T$ is the nodal displacement of the *i*th node, $\left\{d_e\right\} = \left\{\left\{d_1\right\} \quad \left\{d_2\right\} \quad \ldots \quad \left\{d_{n_d}\right\}\right\}^T$ is the displacement vector of the entire element and $\left[N\right]$ is the matrix of shape functions:

$$\left[N\right](x,y) = \left[\left[N_1\right](x,y) \quad \left[N_2\right](x,y) \quad \ldots \quad \left[N_{n_d}\right](x,y)\right] \tag{8.26}$$

In equation (8.26), $\left[N_i\right]$ represents a sub-matrix of shape functions [2]:

$$\left[N_i\right](x,y) = \begin{bmatrix} N_{i1} & 0 & 0 & 0 \\ 0 & N_{i2} & 0 & 0 \\ 0 & 0 & \ldots & 0 \\ 0 & 0 & 0 & N_{n_d} \end{bmatrix} \tag{8.27}$$

where N_{ik} is a scalar shape function related to the *i*th node (usually the same for all $k=1,2,..,n_f$) that we know from before.

Applying the same procedure to a weak form, as before in the FEM analysis of the electromagnetic fields, the system of linear equations is obtained. The unknown vector in this system is the displacement vector. Thus, the weak form (8.24), on an elemental level, reduces to the following matrix equation [2]:

$$\left[k_e\right]\left\{d_e\right\} + \left[m_e\right]\left\{\ddot{d}_e\right\} = \left\{f_e\right\} \tag{8.28}$$

where $\left[k_e\right]$ is the *stiffness* matrix, $\left[m_e\right]$ is the mass matrix and $\left\{f_e\right\}$ is the element force vector acting on the nodes of the element. The elemental mass and stiffness matrices have the following form [2]:

$$\left[m_e\right] = \int_{(S_e)} \rho \left[N\right]^T \left[N\right] dS \tag{8.29}$$

$$\left[k_e\right] = \int_{(S_e)} \left[B\right]^T \left[C\right]\left[B\right] dS \tag{8.30}$$

where $\left[B\right] = \left[L\right]\left[N\right]$ is the so-called *strain matrix.*

The global system of equations is assembled by adding the integral contributions (8.28) of the entire mesh covering our computational domain and it has the following form [1]:

$$[K]\{D\}+[M]\{\ddot{D}\}=\{F\} \tag{8.31}$$

where $[K]$ is the global stiffness matrix, $[M]$ is the global mass matrix, $\{D\}$ is a vector of all the displacements at all the nodes in the entire computational domain, and $\{F\}$ is a vector of all the equivalent nodal force vectors.
The obtained system of equations forms a sparse matrix of a similar structure to those shown in the previous chapter on FEM in electromagnetics.

8.4. FEM Static 2D Analysis of Capacitive MEMS Switch

Mechanical static analysis plays an important role in the design of the so called micro-electro-mechanical systems (MEMS). There are various types of MEMS devices such as thermal based microsensors, photon detectors, microsensors for magnetic field, mechanical microsensors, chemical microsensors, microfluidic systems, biomedical systems, microactuators, micromachines etc. One common characteristic of all the mentioned systems is an extremely small size which is on the order of micrometers. Therefore MEMS devices are considered to be the smallest functional machines engineered by humans [3]. Due to their small size and mass, MEMS devices can reliably and accurately operate in hostile environments such as ones with sever and frequent mechanical shocks, vibrations and so on. Small dimensions, i.e. small masses make possible the production of ultra-fast devices with reaction time far beyond the limit of conventional design. For the same reason, the power consumption and losses of MEMS devices are of a negligible level. The size of mechanical components in typical MEMS is so small that they can be fabricated together with the accompanied electronics on the same silicon substrate, which brings the compact device to levels of reliability previously unimaginable [3].
As an example we will now analyze a shunt capacitive MEMS switch operating at the microwave frequency range [4]. The geometry of the switch is given in Figure 8.2. The switch consists of a thin metal membrane (yellow color) suspended over the center conductor (blue color) of a so-called coplanar waveguide (CPW) [5, 6]. A CPW is a structure containing three parallel conductors at a certain distance. The two conductors on the sides are grounded (red color) and the center conductor (blue color) is connected to the signal source. Everything is made on top of a low-conductivity silicon substrate (green color). As one can see in Figure 8.2, the idea is very simple. At a certain position of the CPW the thickness of the center conductor is reduced, making space for the metallic membrane connected with the grounded conductors on either side. When DC voltage is applied to the center conductor, the electrostatic force acts on the membrane which deforms, touching the dielectric coating of the lower electrode of the switch. Due to its elasticity, the membrane will recover after the DC voltage is removed, i.e. it will move back in the initial position over the lower electrode (center conductor). Thus we have elegantly obtained a device with an *on-* and *off-state*, i.e. we have a switch. The state of the switch is managed from outside by using DC voltage. To estimate the needed DC voltage as well as the dimensions of the membrane, among other things, we have to perform a static mechanical analysis of the structure.
The chosen material for the membrane is aluminum. According to reference [7], aluminum has the following properties that are important for mechanical analysis: $E=6.8\cdot10^{10}Pa$ *(Young's modulus)*, $\nu=0.35$ *(Poisson's ratio)*, $\rho=2698.9\ kg/m^3$ *(density).* If we have a look at the structure in Figure 8.2, it is possible to see that the length of the membrane in the direction parallel to the axis of the CPW ($k=120\mu m$) is much larger than its thickness ($l=0.4\mu m$).

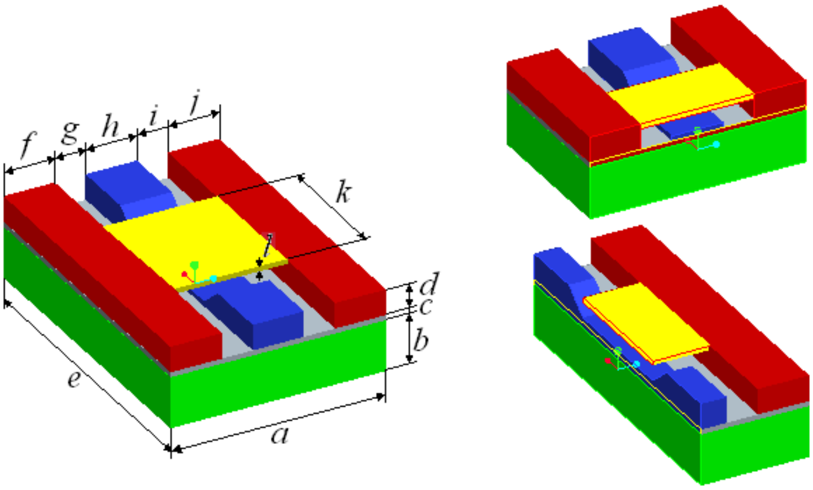

Figure 8.2. Geometric configuration of the shunt capacitive MEMS switch is depicted on the left-hand side; Two major cross-sections are shown on the right-hand side; Depicted dimensions have the following values: *a=520μm, b=600μm, c=1μm, d=4μm, e=600μm, f=h=j=120μm, g=i=80μm, k=120μm, l=0.4μm*; More details are given in the text.

Therefore we can simply perform a 2D *plain strain* mechanical simulation of the membrane and still be accurate in our prediction of the switch behavior from the mechanical viewpoint. In Figure 8.2 on the right hand side (upper part), the cross-section is presented that is valid for our plain strain 2D simulation. A detailed definition of the 2D plain strain model is given in Figure 8.3.

As shown in Figure 8.3a, at the bottom of grounded conductors we have defined fixed boundaries with the prescribed displacement equal to zero. Our electrostatic force acts on the bottom surface of the membrane. Therefore, we have defined the surface force over this boundary.

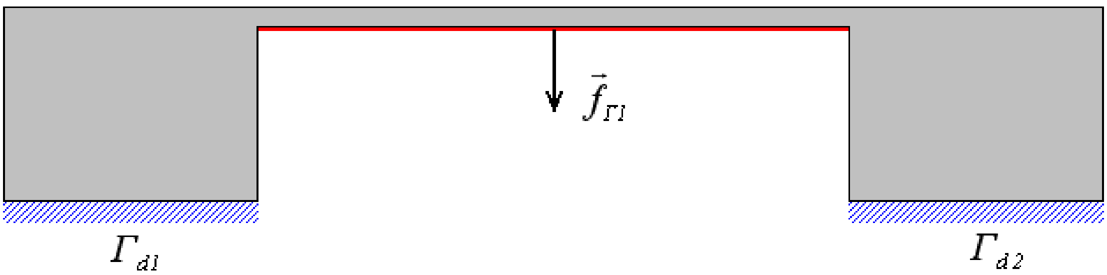

(8.a)

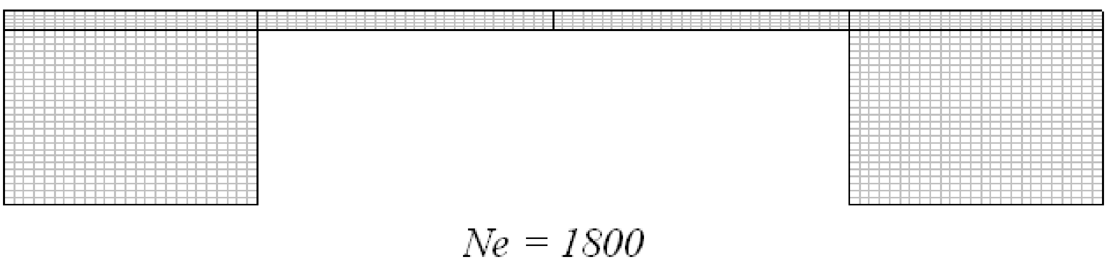

(8.b)

Figure 8.3. 2D plain strain analysis of the MEMS switch presented in Figure 8.2; Boundary conditions (constraints) and loads (surface force) are shown (a); Quadrilateral (regular) mesh is depicted (b); More details are given in the text.

Since our structure has a large disproportion between its width (*520μm*) and height (*4μm*), the visualization of the geometry in Figure 8.3 is significantly scaled in the y-direction to be able to see the details of the picture. Moreover, such a large disproportion produces problems for mesh generators and then numerical difficulties for the field solver (ill-conditioned matrices). Therefore, we have used the regular quadrilateral mesh presented in Figure 8.3b.
To estimate the force needed for the membrane pull-in, we have performed several plane strain calculations on the geometry given in Figure 8.3a for various surface forces. The results are presented in Figure 8.4.
In Figure 8.4 the color shadows represent the stress in the structure and the colorbar at the top of each picture shows corresponding values. The position of the deformed geometry is related to the calculated displacement.

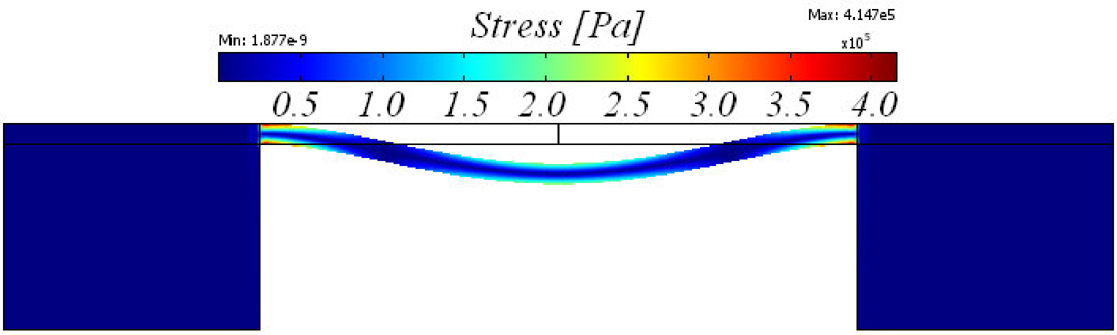

$$\vec{f}_{\Gamma 1} = 0 \cdot \vec{e}_x - 2 \cdot \vec{e}_y$$

(8.a)

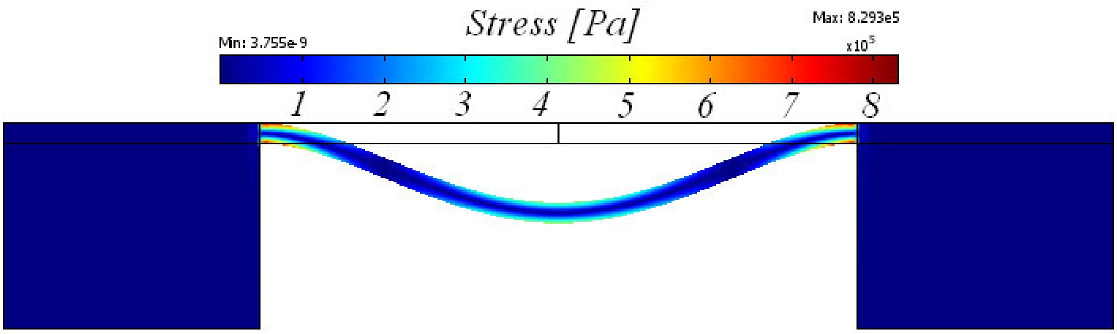

$$\vec{f}_{\Gamma 1} = 0 \cdot \vec{e}_x - 4 \cdot \vec{e}_y$$

(8.b)

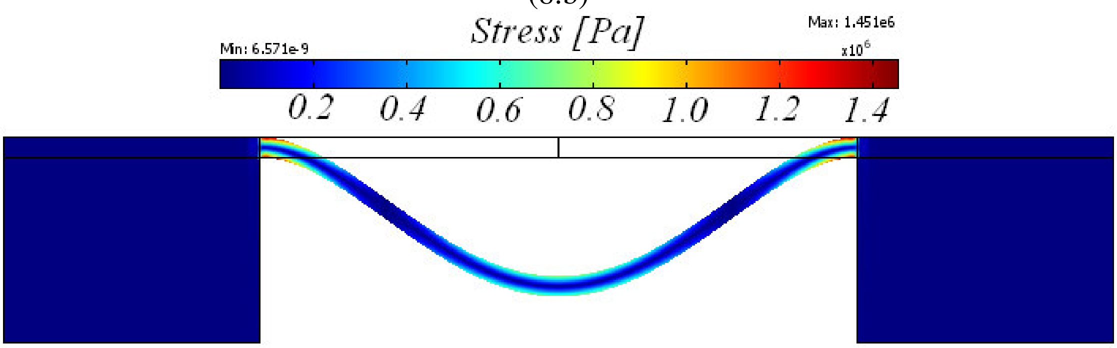

$$\vec{f}_{\Gamma 1} = 0 \cdot \vec{e}_x - 7 \cdot \vec{e}_y$$

Figure 8.4. Results of the 2D plain strain analysis of the MEMS switch presented in Figure 8.2 for various values of the surface force acting on the bottom of the membrane; Stress is presented as colour fill and the deformed position of the elements of the membrane represent the displacement; Original edges of the geometry are given as black solid lines.

The geometry of the no-load body (the surface force equal to zero) is given with the black solid lines. Thus, for various forces, one can see the severity of the deformation. Apparently, a larger force will produce more significant bending of the membrane. By increasing the force, one can estimate the value of the surface force needed to pull-in the membrane, i.e. needed to change the state of the switch from *off* to *on*. As it will be shown later, this is only a rough estimation because the displacement of the membrane causes a change in the electrostatic field and consequently a change of electrostatic force. Very accurate estimations of the pull-in force can only be done if we perform the so-called coupled electrostatic-mechanic analysis, which will be the subject of Chapter 11.

8.5. FEM Eigenvalue 2D Analysis of Capacitive MEMS Switch

If the system of equations (8.31) has a total number of degrees of freedom (DOFs) equal to *N*, then the stiffness matrix $[K]$ and mass matrix $[M]$ have dimensions of NxN. The displacement vector is obtained as a solution to (8.31). Using the displacement, the stress and strain can be calculated. The question is: what to do in the case when *N* is very large? An alternative way of solving (8.31) is the so-called mode superposition technique. In this approach, one has to solve the associated eigenvalue problem of equation (8.31). Namely, the eigenvalue problem can be obtained from (8.31) when the load is equal to zero, i.e. $\{F\}=0$. Thus, the system of equations (8.31) becomes a homogenous system and its analysis is therefore called *free vibration analysis* [1]. The homogenous form of (8.31) reads:

$$[K]\{D\}+[M]\{\ddot{D}\}=0 \tag{8.32}$$

If the free vibrations are assumed to be harmonic in time, the unknown displacement vector can be written as follows:

$$\{D\}=\{\phi\}\cdot e^{j\omega t} \tag{8.33}$$

where ω is the angular frequency of the free vibration, t is the time and $\{\phi\}$ is the amplitude of the nodal displacement. By combining equations (8.33) and (8.32) it is possible to write:

$$\left([K]-\omega^2[M]\right)\{\phi\}=0 \tag{8.34}$$

or in a more suitable form:

$$\left([K]-\lambda[M]\right)\{\phi\}=0 \tag{8.35}$$

where $\lambda=\omega^2$. Equation (8.35) is called the eigenvalue equation. It is well known from linear algebra [8] that the non-trivial (non-zero) solution of the homogenous linear system of equations is possible only if the determinant of the system is equal to zero:

$$\det\left([K]-\lambda[M]\right)=\left\|[K]-\lambda[M]\right\|=0 \tag{8.36}$$

The left-hand side of equation (8.36) is obviously a polynomial in terms of λ and the order of the polynomial is equal to the size of the system N. In general this polynomial equation has *N* roots $\lambda_1,\lambda_2,...,\lambda_N$ called *eigenvalues*. The eigenvalues of system (8.31) are the natural frequencies (eigen-frequencies) of the analyzed solid body. Each eigenvalue λ_i has its corresponding eigenvector $\{\phi_i\}$ forming a so-called eigen-pair. A corresponding eigenvector can be calculated from (8.36) as follows:

$$([K]-\lambda_i[M])\{\phi_i\}=0 \tag{8.37}$$

The eigenvector $\{\phi_i\}$ represents the i-th vibration mode, i.e. the shape of the vibrating structure of the i-th resonant frequency.

The practical importance of the eigenvalue analysis can be seen from the fact that an applied dynamic load with a frequency that equals a natural frequency of the structure can produce extremely violent vibrations which usually lead to the collapse of the structural system. Therefore, the information on the natural frequencies of a structure are of paramount importance for every mechanical system.

The results of the eigenvalue analysis of the MEMS switch from Figure 8.3 are given in Figure 8.5. It is possible to see that the mass of the membrane is so small that its vibrations can not affect the conductors of the CPW. The plot of the displacement is not realistic and it has been scaled to the values needed for nice visualization. If we increase the size of the structure, the eigenfrequencies decrease and vibrations of the CPW conductors become much more severe as shown in Figure 8.6.

It is obvious that the eigenvalue analysis can give us important information about the dynamic properties of a MEMS device and its switching speed or frequency. In order to have a reliable operation of the switch, the switching frequency should be far from any natural or resonant frequency of the device.

8.6. Concluding Remarks

In this chapter the FEM mechanical analysis in its simple 2D version has been presented. Apparently, the FEM approach is very similar to its equivalent in electromagnetics. The starting equations are naturally different (different physics) but the algorithm of their FEM discretization is very similar. Furthermore we have seen the importance of mechanical analysis from the micro- and nano-viewpoint. Through the MEMS example we have shown that the design of such devices needs a static mechanical analysis as well as an eigenvalue (free vibrations) analysis. It will be shown later that an accurate analysis of the presented MEMS switch can be preformed only with a full coupling of mechanics with electrostatic analysis. This will be a final step where we need to combine several different analyses in order to accurately predict the behavior of the device.

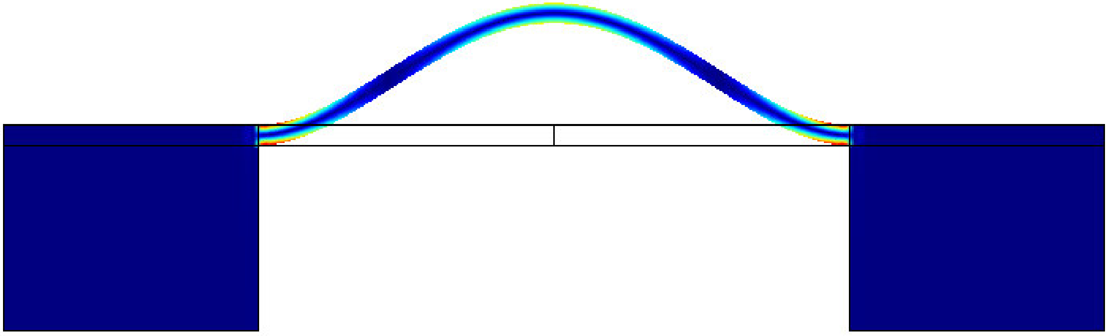

$f_1 = 8902.79\,Hz$

(8.a)

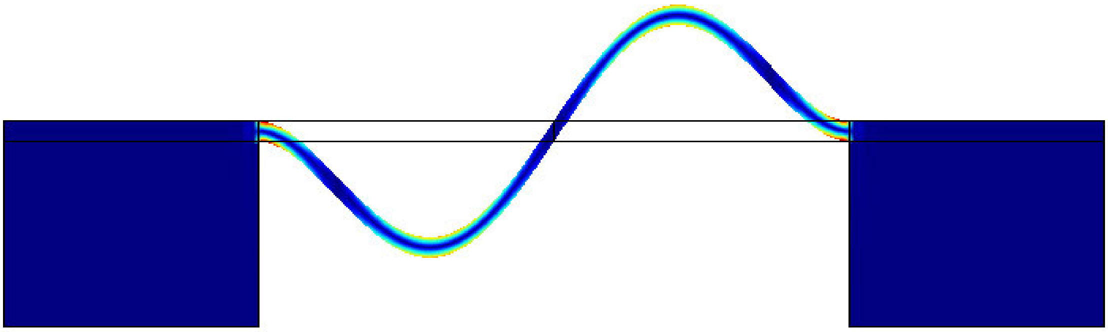

$f_2 = 24569.72\,Hz$

(8.b)

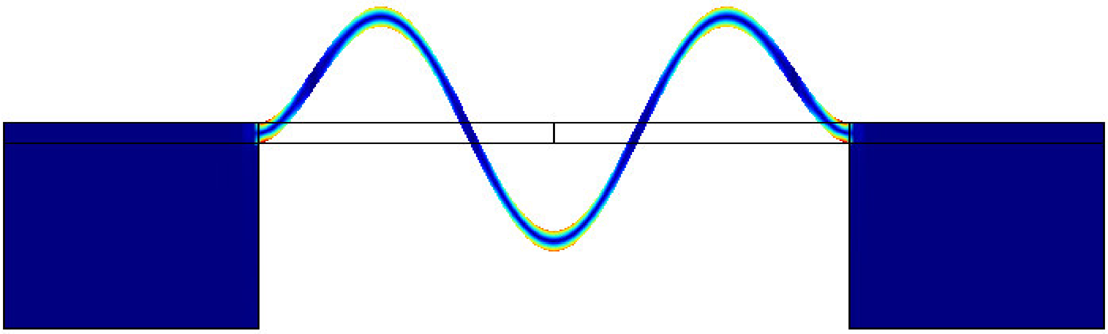

$f_3 = 48242.12\,Hz$

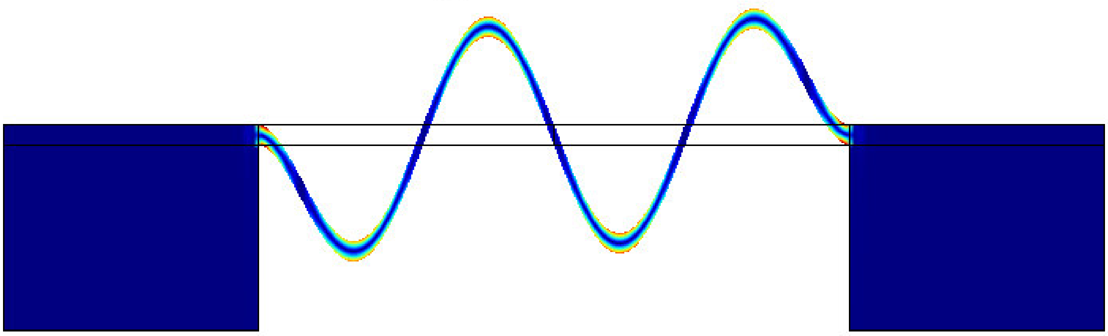

$f_4 = 79905.75\,Hz$

Figure 8.5. Results of the 2D plain strain eigenvalue analysis of the MEMS switch presented in Figure 8.2; The first 4 eigenpairs are shown; Stress is presented as colour fill and the deformed position of the elements of the membrane represent the displacement; Original edges of the geometry are given as black solid lines; Corresponding eigenfrequency is given at the bottom of each figure.

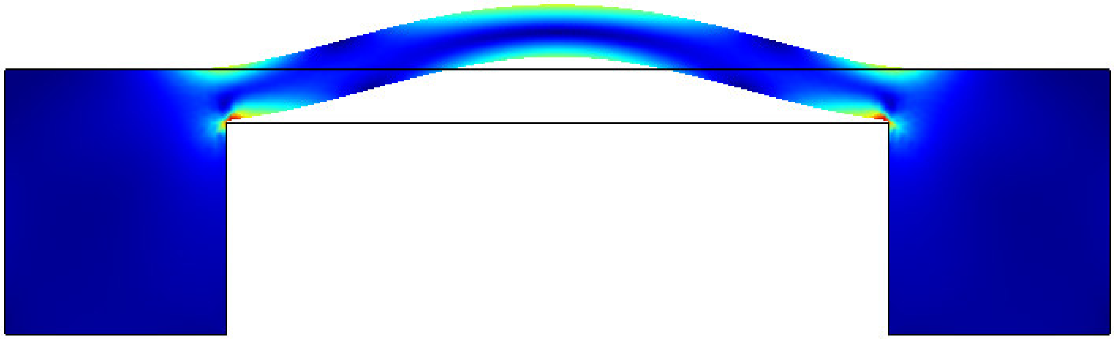

$f_1 = 303.41Hz$

(8.a)

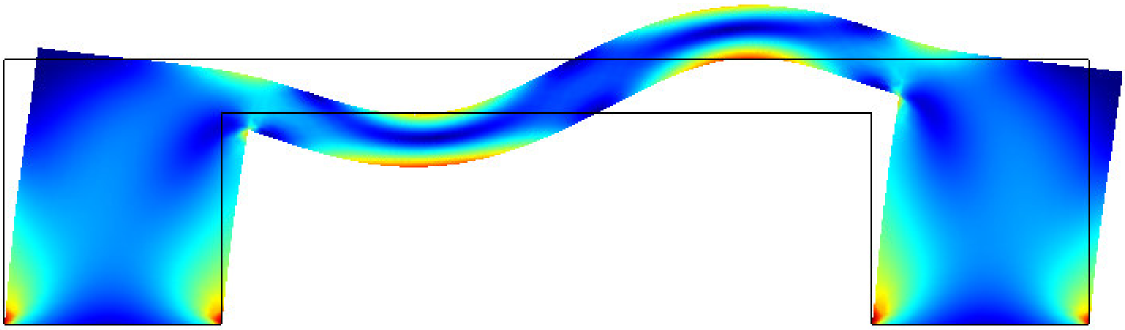

$f_2 = 666.07Hz$

(8.b)

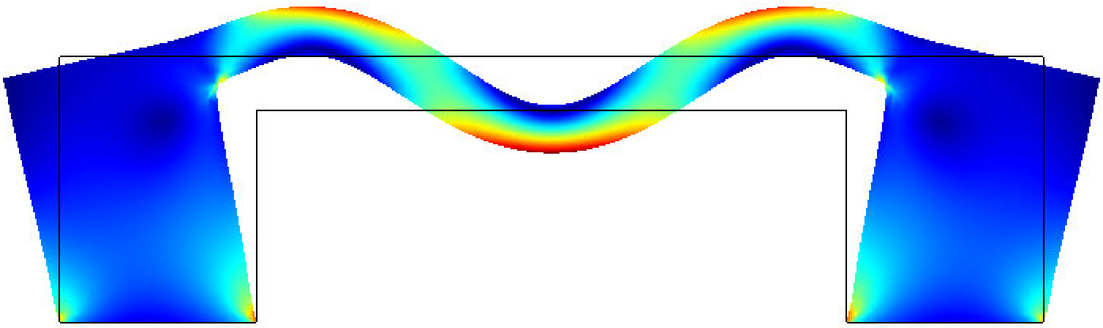

$f_3 = 1311.92Hz$

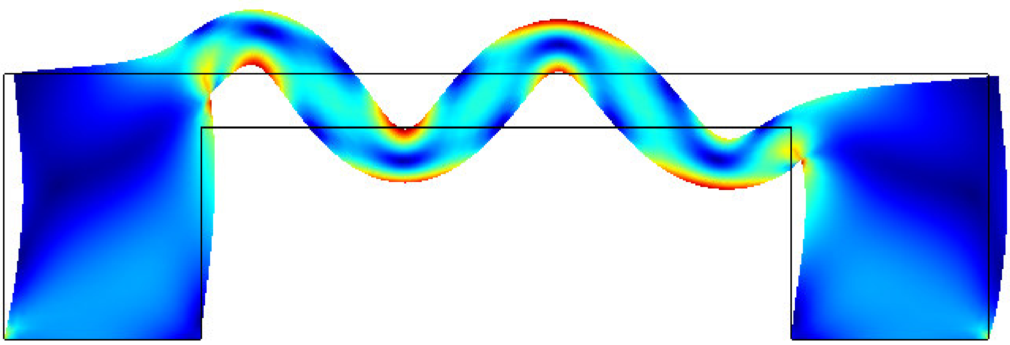

$f_4 = 2112.82Hz$

Figure 8.6. Results of the 2D plain strain eigenvalue analysis of the larger structure (size has been increased in order to produce more sever vibrations); The first 4 eigenpairs are shown; Stress is presented as colour fill and the deformed position of the elements of the membrane represent the displacement; Original edges of the geometry are given as black solid lines; Corresponding eigenfrequency is given at the bottom of each figure.

8.8. References

[1] G. R. Liu, S. S. Quek, "The Finite Element Method: A Practical Course", Elsevier Science Ltd., Oxford, Amsterdam, Boston, London, Tokyo, 2003.
[2] F. Kreith, D. Yogi Goswami Eds., "The CRC Handbook of Mechanical Engineering", the Second Edition, CRC Press, Boca Raton, USA, 2005.
[3] J. G. Korvink, O. Paul, Eds., "MEMS: A Practical Guide to Design, Analysis, and Applications", William Andrew Publishing and Springer Verlag GmbH, Norwitch, NY, 2006.
[4] J. Y. Qian, F. De Flaviis, G. P. Li, "Finite Element Model of Microelectromechanical Systems Switch Operating at Microwave Frequencies", Final Report 1998-99 for MICRO Project 98-083, Department of Electrical and Computer Engineering, University of California, Irvine, CA, 1999.
[5] C. P. Wen, "Coplanar Waveguide: A Surface Strip Transmission Line Suitable for Nonreciprocal Gyromagnetic Device Applications," IEEE Trans. Microwave Theory Tech., Vol. 17, No. 12, pp 1087-1090, 1969.
[6] R. N. Simons, "Coplanar Waveguide Circuits, Components, and Systems", John Wiley & Sons, New York, Singapore, Toronto, 2001.
[7] MatWeb - The Online Materials Information Resource, www.matweb.com.
[8] G. H. Golub, Ch. F. Van Loan, "Matrix Computations", 3rd Edition, The Johns Hopkins University Press, Baltimore, 1996.